Journal of Urban Mobility 1 (2021) 100003

Contents lists available at ScienceDirect

Journal of Urban Mobility

journal homepage: www.elsevier.com/locate/urbmob

Design of indicators to guide capacity improvements in urban railway lines

L.M. Navarro [a,*], A. Fernandez-Cardador [b], A.P. Cucala [c]

[a] Siemens Rail Automation S.A.U., Cornellà de Llobregat, Spain
[b] Institute for research in technology, ICAI School of Engineering, Comillas Pontificial University, Madrid, Spain
[c] Institute for research in technology, ICAI School of Engineering, Comillas Pontificial University, Madrid, Spain

ARTICLE INFO

Keywords:
Urban transport
Dwell times
Capacity
Railway
Indicators

ABSTRACT

The transport capacity of an urban railway line can be increased in many different ways. For planners and infrastructure managers it is vital to have all the tools available that allow choosing the most cost-effective solution among all the possibilities. This selection process can be complex sometimes and deciding how the available capacity should be increased is an important decision with significant financial consequences.

In this paper new transport capacity indicators suitable for urban lines are presented; that can be used as a guide by decision-makers to help them decide on infrastructure capacity improvements. The indicators ease the process of deciding among different alternatives by considering the specific capacity improvement they involve individually.

The model uses a railway simulator that allows obtaining the minimum departure-arrival itinerary times in the station under study. It has been applied to a case study in a suburban commuter line in Barcelona. Specifically, to the station of Provença that is a station with long Dwell Times during rush hour and belonging to the Spanish railway operator FGC.

This case demonstrates the indicators application and contributions; it also shows that it would be possible to extend the same kind of study to other nodes allowing the systematization of their capacity improvement by fine-tuning their signaling system.

1. Introduction: capacity improvements in urban railway lines

The demand for urban transport will increase in 95% until 2050, especially in developing countries where cities are expected to growth hugely in size. Urban dwellers will rise from 4 to 6.4 billion people during the aforementioned period (OECD, 2017).

Railway is one of the most efficient modes of urban public transportation and it has seen an impressive technological improvement during the last few decades. Looking into the future, railway is expected to be a cornerstone to alleviate congestion problems in big cities and metropoles all around the globe.

Specifically, demand for railway urban transport is expected to increase 60% and this rise will put a lot of pressure on current infrastructure. Therefore, city planners and infrastructure managers will have to take complex decisions in order to increase the capacity of current railway networks. Building completely new infrastructure as well as the use of different rolling stock that allow more capacity are options on the table, but they are quite expensive ones. Also, they tend to be constrained by political momentum and funding, the rhythm of which is usually not synchronized with social needs.

But, before engaging in lengthy and costly upgrading processes, there are other easier and convenient options that need to be analyzed. Transport capacity limitations in railway networks are caused to a great extent by high dwell times at stations especially in high density urban lines. These dwell times at stations can be harmful to capacity availability particularly during the rush hour when a great number of passengers make use of the service. An extended dwell time for a particular train can disrupt the following one; that train will have to reduce its speed or even come to a complete stop. This situation happens because the minimum departure-arrival itinerary times (I_{DAmin}) required between trains following each other are not fulfilled, and then the following train is too close to the previous one and its movement gets disrupted. So, it becomes key to improve the departure-arrival itinerary times at the station in order to improve the capacity at each of them. This is the main contribution of this work and it represents a new take on railway capacity improvement.

* Corresponding author.
E-mail addresses: luismiguel.navarro@siemens.com (L.M. Navarro), antonio.fernandez@iit.comillas.edu (A. Fernandez-Cardador), cucala@comillas.edu (A.P. Cucala).

https://doi.org/10.1016/j.urbmob.2021.100003
Received 27 October 2020; Received in revised form 20 June 2021; Accepted 15 July 2021

I_{DAmin} represents the minimum interval corresponding to the time passed between the start of the movement of the first train from a station until the stop in the same station of a following train without any disturbance caused to the second train by the signaling system. So that an increase of one more second in the moment of departure of the first train would start causing disruption to the following train.

In the railway environment different types of capacity are typically used (Abril et al., 2008). Theoretical Capacity (see Eq. (1)) is the maximum value that could be obtained in a line under ideal conditions without any existing delays. Practical Capacity considers some additional buffer times that are introduced in the timetable to absorb possible delays so that a more realistic measure of line capacity is offered. But it is still a fixed value that does not fully account for disruptions and delays since it considers that trains are not disrupted by the signaling system.

However, during real line operation in urban lines traffic can be heterogeneous and service disruptions and delays are often suffered. These disruptions are quite common during the rush hour in urban lines close to saturation; therefore, it is necessary to take these situations into account when it comes to system design.

In the aforementioned situation, trains travel in disrupted conditions caused by the signaling system and the measures of Theoretical and Practical Capacity of the line are not useful anymore since these measures are not enough to account for slowdowns caused by the signaling system that control the flow of trains throughout the line. Therefore, it is necessary to define new Capacity Indicators for urban lines that are useful to characterize urban railway installations where it is frequent to have trains travelling in disturbed conditions. The definition of this new Capacity Indicators is the challenge addressed by the present work.

The following parts of the paper are organized as follows. A revision of state of the art of the literature is shown in Section 2. A Model to calculate disturbed capacity indicators using a rail simulator and real data coming from the actual installation is presented in Section 3.1. the developed Model and its resolution are presented in Section 3.3. The obtained results and discussion are shown in Section 4. And finally, Section 5 is dedicated to the conclusions of the paper.

2. Literature

Some authors present different methods to evaluate between several transport improvement alternatives like Nalmpantis et al. (2019) who present an application of a Multi-Criteria Decision Analysis (MCDA) method: The Analytic Hierarchy Process (AHP). That method is based on expert's evaluation to allow deciding among different transport implementations.

For its part, Luteberget et al. (2019) present a verification technique and tool to be used at the design phase of the installation to assess its capacity; this allows processing different design solutions to choose the optimal one.

In Haramina and Talan (2018) the feasibility of a new timetable solution in a suburban line to be expanded from single to dual-track line is validated. They perform several iterations in station areas to obtain the desired results and also applied different simulation scenarios to validate their conclusions.

In Burdett (2016) is presented an analytical model suitable to identify capacity expansions in railway systems considering track duplications and subdivisions of sections. The model allows to decide in each case which design approach is more effective and also is of application to new railway networks.

In Ljubaj et al. (2017) the authors present an analysis of the bottlenecks of a line with the aim of increasing its capacity utilization without resorting to expensive new investments. The use of a simulator allows the assessment of different situations and changes in the infrastructure. Ljubaj et al. (2018) displays a similar approach allowing the selection and discard of different line upgrade alternatives according to their justification in terms of capacity increase. In Ljubaj et al. (2019) a double-track line and its planned upgrade to allow for bi-directional traffic are analyzed and simulated in order to assess the economic feasibility of the line upgrade.

Macroscopic models used to analyze the future capacity of networks using forecast data are presented in Reinhardt et al. (2018). The models can be used to find bottlenecks under different demand scenarios and to choose between a set of possible capacity expansions, helping proper placement of future railway infrastructure investments.

In Jensen et al. (2017 a model to calculate railway infrastructure occupation and capacity consumption by using a stochastic simulation of delays is presented. It is applied to different scenarios and it does not require a timetable, allowing optimization of the infrastructure by considering different train sequences.

Additionally, several works have been published related to the modelling of disturbed railway systems. In Abril et al. (2008) the authors show a summary of the different methods available to calculate railway capacity; also, it shows some simulation methods that allow the reproduction of train interactions and knock-on delays. In Huang et al. (2019) the authors review the disturbances in high-speed lines and considering train interval, disturbance length, occurrence time and disturbance influence; they present a model based on K-Means clustering that allows analyzing disturbances in real-time operation.

A mesoscopic simulation method that allows calculating values of capacity at stations is proposed in Zhong et al. (2018). It also considers the presence of random disturbances although only of train and operation delays.

In Zieger et al. (2018) the authors present a simulation model to analyze the influence of buffer times distributions on capacity and level of service (expected waiting time for trains). The model is also compared to the STRELE framework to assess its validity and differences.

An approach to simulate a single direction suburban railway system based on the Nagel-Schreckenberg model is showcased in Becker and Schreckenberg (2018). This approach uses a cellular automaton with the application of stochastic dwell times; this was previously used to reproduce jamming effects in roads.

In Shekhar et al. (2019) the authors demonstrate a railway junction simulator with mixed traffic based on Python. It uses graph theory to simulate the junction and select the best path available to traverse it and identify existing bottlenecks. It also allows comparing the effects of changes in the infrastructure.

The concept of dynamic capacity consumption is introduced in Goverde et al. (2013); random distributions of delays are used to model real-life operations to simulate disturbed conditions. A modular dispatching system based in a microscopic model of the line under test is shown.

In Gašparík et al. (2018) a simulator based on RailSys is presented. It allows simulating railway lines with mixed traffic and introducing different delays into the system with the aim of calculating the line capacity value.

In this paper, indicators designed to guide capacity improvements in urban lines with high occupancy stations are presented. Their specific goal is the removal or impact reduction of bottlenecks in stations that reduce the overall capacity of the line. Also, the presence of service disruptions due to hindered circulations during the rush hour and their effects has been considered in the indicators design.

These novel indicators ease the decision-making process required when it comes to making investments on the infrastructure to guide capacity enhancements. When different scenarios are presented to the infrastructure manager, having the proper tools to choose among them results in a long-term very valuable asset.

3. Disturbed capacity model

3.1. Model description

In this section, a model to calculate disturbed capacity indicators using a rail simulator and real data coming from the actual installation

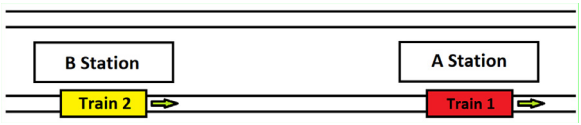

Fig. 1. Disturbance measurement for two consecutive trains.

is proposed. The Theoretical Capacity associated to the passage of trains in trains per hour through a station of a metro line is obtained as:

$$C = \frac{3600}{H_{min}} \quad (1)$$

Where:

$H_{min} = I_{DAmin} + DT$ [s]
DT: Dwell Time [s]
I_{DAmin}: Minimum interval for 2 trains at a station [s]
H_{min}: Minimum Headway [s]
C: Theoretical Capacity [t/h]

This model allows considering disturbances in nodes and the process of choosing between different signaling solutions.

This model uses as a measurement of disturbance between two consecutive trains considering the time of departure of those two trains from two consecutive nodes (A and B):

$$T_{BT} = T_{BTP} - (T_{D2B} - T_{D1A}) \quad (2)$$

Where:

T_{D1A} = Time of departure of 1st train from station A
T_{D2B} = Time of departure of 2nd train from station B
T_{BTP} = Limit of difference between departure times of two trains from two consecutive nodes; times lower than this value imply a disturbance to the movement of the second train
T_{BT} = Difference of Departure Times between two consecutive trains from two consecutive stations

During nominal performance trains depart from the station B and arrive to station A without being disturbed through the signaling system by any previous train, with T_{D2B}-T_{D1A}>T_{BTP}. As T_{D2B}-T_{D1A} gets reduced the following train of the pair starts to be disturbed by the previous one (T_{D2B}-T_{D1A})<T_{BTP} and T_{BT}>0. This situation is presented when for example Train 1 increases its dwell time at the station B. Therefore, the T_{BT} value when positive shows that two trains are running under their limit of disturbance and its value denotes for how many seconds that limit is being surpassed. So, it is a measurement of disturbance between two consecutive trains.

The following chart shows the running time between the departure of a train from Station B and its arrival to Station A as a function of the increase in Dwell Times beyond the point when the movement of the second train gets disturbed by the first one in Station A. For values of T_{BT} smaller than 0 the time of movement of the second train is constant since the movement of the train is not hindered by the signaling system because there is enough distance between both trains to run without disturbing each other.

From T_{BT} > 0 the movement of the second train is affected by the signaling system, increasing therefore its time of movement. In T_{BT} = 0 the Theoretical Capacity value can be found, that is the Capacity value that allows trains to move as close as possible without affecting each other. In this point the difference between the departure of the first train from A Station and the arrival of the second one to the same station is I_{DAmin}, which offers the minimum headway without disturbance.

Note that when the T_{BT} value reaches a certain value the train suffers a complete standstill due to the action of the signaling system (Fig. 2, t of 32s). After this value the graph of running time is a straight line with an angle of 45º, because for every extra second of T_{BT} the train is stopped one more second due to the action of the signaling system

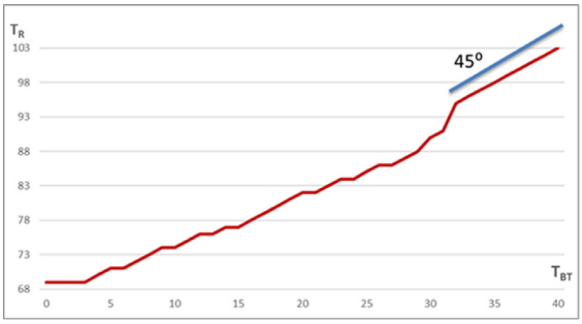

Fig. 2. Train 2 running time (y-axis) versus increase of dwell time of train 1 (x-axis) after the T_{BTP} limit values.

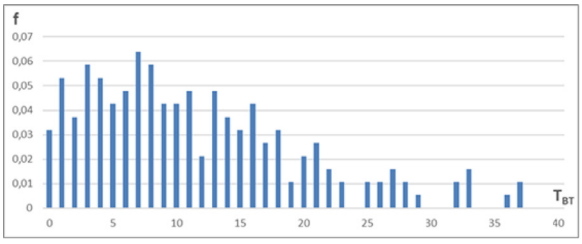

Fig. 3. Example of normalized statistical frequency of T_{BT} > 0 accumulated values (y-axis) versus Increase of Dwell Time of Train 1 (x-axis) after the T_{BTP} limit value.

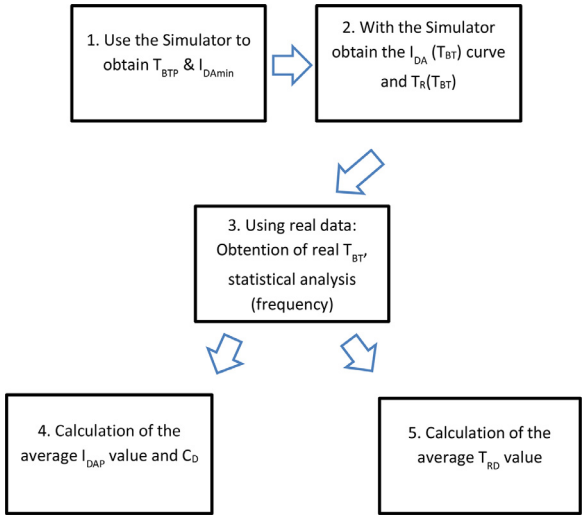

Fig. 4. Model flow chart.

that stops it for one additional second. This increases for one second its running time to the next station.

For values of T_{BT} higher than 0 the values of Theoretical Capacity are not useful anymore because the trains are moving in disturbed conditions. As an evolution to Eq. (1), in those situations where T_{BT} is higher than 0 the new indicator of Disturbed Capacity is defined as:

$$C_D = \frac{3600}{H_D} \quad (3)$$

where:

HD = I_{DAP} + DT
DT: Dwell Time
I_{DAP}: Average Disturbed Interval
HD: Average Disturbed Headway

I_{DAP} is the average value of the disturbed departure-arrival interval, it can be calculated as the expected value of the statistical distribution

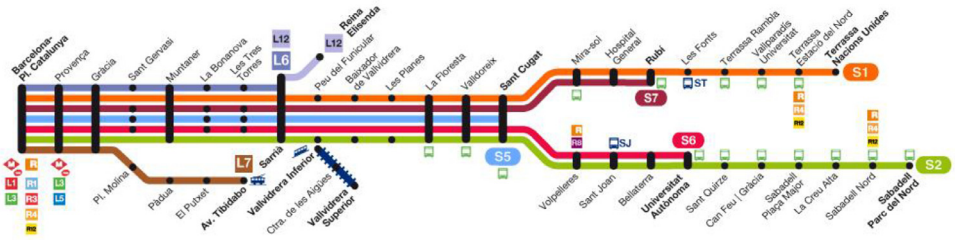

Fig. 5. Map of FGC Barcelona-Vallès line.

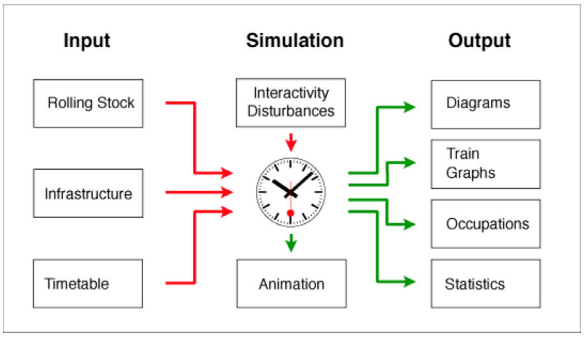

Fig. 6. Simulator operation process.

of I_{DA} for values of T_{BT} >0. This distribution is produced during the real service of the line during the period of time under analysis (for example during the rush hour). H_D is the average disturbed headway value between trains that are moving under disturbed conditions and C_D is the disturbed Capacity value associated to the installation under those disrupted circumstances.

The expected I_{DAP} value is obtained using:

$$I_{DAP} = \int_0^{INF} I_{DA}(T_{BT}) \times f(T_{BT}) d(T_{BT}) \quad (4)$$

Where $f(T_{BT})$ represents the statistical frequency of the disturbances (variable T_{BT} for $T_{BT} > 0$) experienced during the time period of the real line service under analysis. $I_{DA}(T_{BT})$ is the interval between departure and arrival of two consecutive trains to a station produced for every value of T_{BT}. $f(T_{BT})$ is also obtained using statistical analysis of real data during the time zone under study to consider the level of disturbance of the trains approaching the station. This level of disturbance in the station under analysis depends also on the level of disturbances in the following stations of the line that may generate a ripple effect down the line.

$I_{DA}(T_{BT})$ depends only on the signaling system and the train speed profile and for an existing installation that can be obtained using statistical analysis of train movements real data. In the cases of greenfield or resignaling projects simulation tools can be used to calculate and evaluate Capacity indicators under disturbed conditions. In Fig. 9 an example of $I_{DA}(T_{BT})$ is presented; the straight part of the graph after 33 seconds of T_{BT} corresponds to values of dwell time of train 1 that actually cause train 2 to come to a complete stop.

The second indicator of the line under disturbed conditions is the loss of commercial speed caused by the speed reduction generated in the signaling system. The indicator related to the Disturbed Running Time (T_{RD}) is obtained as the expected value of running times T_R when movements are disturbed, T_{BT} is higher than 0 and the frequency of real disturbance of trains f is known.

$$T_{RD} = \int_0^{INF} T_R(T_{BT}) \times f(T_{BT}) d(T_{BT}) \quad (5)$$

$T_R(T_{BT})$ depends on the signaling system, the train speed profile and on the frequency of disturbed trains arriving to the station. For an existing installation it can be obtained using statistical analysis of real data of train movements. In the cases of greenfield or resignaling projects simulation tools can be used to calculate and evaluate it.

In conclusion, two indicators associated to periods involving disturbed trains moving between two nodes have been presented: C_D and T_{RD}. The first one is a measurement of disturbed capacity while the second measures the loss of service quality produce under these situations. Both indicators need to be considered to design and redesign signaling systems; a reasonable compromise must be achieved.

3.2. Model steps

In this section the procedure to apply the proposed model is presented. The model requires the following steps to perform the complete evaluation:

1 The minimum $(T_{D2B} - T_{D1A})$ value (T_{BTP}) that allows unhindered operation and the associated I_{DAP} value are both obtained with the use of the simulator. To accomplish this several 2-train simulations are performed with the goal of launching the second train as close as possible to the first one without its movement being disturbed by the signaling system due to the proximity to the first train.
2 Using the simulator to perform several runs and starting from the T_{BTP} value, the T_{BT} value is increased from 0 in successive simulation steps with the aim of obtaining the $I_{DA}(T_{BT})$ characteristic curve of the node under study. In this step the movement of the second train is always affected by the first one. Then, the I_{DA} curve obtained with all the iterations simulated represents a curve of how the second train is affected by the signaling system as it gets closer to the first one. In the same way, the running times of the second train $T_R(T_{BT})$ are obtained following the aforementioned iterative simulation process.
3 Furthermore, with the analysis of real installation data coming from the operator the frequency of real disturbances is calculated. That is the frequency of the T_{BT} variable. From this data and using the minimum T_{BTP} value that allows unhindered operation found in step 1, the numbers are filtered to obtain the frequency of $T_{BT} > 0$ values that cause the disturbance in the installation during real operating conditions.
4 The average I_{DAP} value is the basis of the indicator of disturbed capacity. This average value is obtained as a result of the weighted average of all I_{DA} values obtained with the simulator weighted by their real occurrence frequency in the node under study for $T_{BT} > 0$. The indicator meaning is clear: it is the average interval considering the real statistical disturbance level existing in the node and it offers information regarding the true level of disturbance experienced in the node. Also, the C_D value is calculated and gives information of the disturbed Capacity Value associated to the installation.
5 The indicator of average disturbed running time T_{RD} is obtained in a similar way to the indicator of disturbed capacity. It is obtained as the average of all disturbed route times (for $T_{BT} > 0$) weighted by their frequency of their occurrence.

Both indicators of Disturbed Capacity and Average Disturbed running Time T_{RD} constitute a useful tool to decide among different signaling alternatives to redesign existing signaling installations.

Regarding Disturbed Capacity C_D it gives precise information about the installation usage under disturbed conditions. This indicator is more

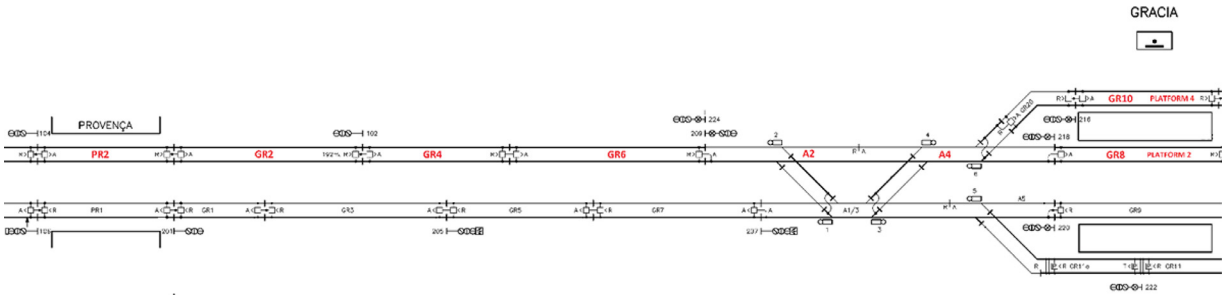

Fig. 7. Track schematic Gràcia – Provença

useful than the Theoretical Capacity one because it considers the interactions between trains; therefore, considering the resulting effects they produce to each other and that are transferred through the signaling system.

The different signaling design alternatives are simulated and then the aforementioned indicators are obtained. The best signaling solution will be the one offering better indicators. This implies a higher level of capacity in real conditions that include disturbed circulations, but at the same time keeping in check the average route time.

3.3. Case study

In this section an example of resolution of the model presented in the previous section is described.

3.3.1. Line description

The FGC Barcelona-Vallès line has been chosen to apply the methods described in the previous sections. FGC (Ferrocarrils de la Generalitat de Catalunya) is a railway company which operates several lines in Catalonia (a region located at the northeast of Spain). And the Barcelona-Vallès line connects Barcelona with the cities of Terrassa and Sabadell going through the Collserola range.

The Barcelona-Vallès infrastructure is fitted with an ATP (Automatic Train Protection) safety system which is in charge of supervising the train speed and applying the penalty brake in the event of safety conditions not being fulfilled. This line is equipped with continuous data transmission through coded track circuits with a speed codes implementation scaled to 90/60/30/0 km per hour. It enforces speed limits and movement authorities ensuring safety of train movements by comparing the current train speed to the permitted speed limit. Speed is limited by the system to protect routes of other trains in the installation or due to other existing constraints in the line.

With the aim of obtaining precise times of the itineraries in the installation, a parametric model of the section has been implemented using a simulation tool. This tool allows modelling line profile data and track topology as well as rolling stock and the routes for each interlocking of the line.

The station of Provença is arguably one of the most congested nodes in the whole network. It is a key station serving several lines: L6, L7, S1, S2, S5, S6 and S7. Hence, it constitutes a perfect testing ground to apply the tools shown in previous sections.

3.3.2. Simulator description

The infrastructure topology of the railway line has been developed in a graphical manner using the OpenTrack tool (Nash & Huerlimann, 2004), which supports modelling a railway line by means of double vertex graphs (Fig. 7). Graphic elements have attributes that can be precisely configured by the user. Also, precise data of the rolling stock such as technical characteristics for every Electrical Multiple Unit including traction efforts and speed diagrams, weight, length, adherence factor and power systems can be introduced. In particular, real data obtained from FGC series 112, 113 and 114 currently in service have been applied.

Signaling and ATP systems have been modeled using real data coming from the installation, such as track circuit lengths and gradients, signals, routes between signals, switches and ATP system features.

3.3.3. Node description

The current Provença station was opened in 1929 and has nowadays a passenger density of 4700 passengers per hour during the rush hour, only surpassed by Plaça Catalunya in the Barcelona-Vallès line. This density is expected to be increased even more during the next years and the station has been remodeled in 2019 to admit this upcoming passenger increment.

3.3.4. Description of the traffic pattern under analysis

The traffic pattern under analysis is formed by the movement of trains between Gràcia and Provença stations towards Plaça Catalunya. Therefore, trains leave Gràcia station alternatively from platforms 2 (GR8) and 4 (GR10).

The movement of trains follows a route through track circuits A4, A2, GR6, GR4, GR2 and PR2 which corresponds to the platform in Provença station. The ATP system implementation follows the design shown in Table 1.

The codes follow the definition XX/YY, where XX is the maximum speed in the current track circuit while YY is the permitted track speed allowed at the end of the current track circuit. The codes received by the second train via the continuous data transmission through the coded track circuits are shown on Table 1. They depend on the track circuits occupied by the previous train; the closer the trains are the more restrictive the speed limits received by the following train become. This is because the signaling system protects the second train route from colliding with the previous route, which means that the following train reduces its commercial speed due to the presence of the previous train and the reduced speed codes it generates after it.

4. Results

4.1. Application of the model steps to the case study

In this section the application of the Model Steps to the Case Study is presented:

Steps 1&2. Obtention of the minimum T_{BTP} (limit of disturbances), I_{DAmin}, $I_{DA}(T_{BT})$ and $T_R(T_{BT})$

In the table below the results obtained out of the simulations performed are presented.

$$T_{BT} = T_{BTP} - \left(T_{D2B} - T_{D1A}\right) \tag{6}$$

The first column shows the increment of Dwell Time of the first train in Provença platform. The second column shows the interval between the departure of the first train and arrival of the second one (I_{DA}). And the third one is showing the running time of the second train; this time displays directly the affectation produced on the second train by the

Table 1
ATP Speed values allowed in section Gràcia – Provença.

Occupied Track Circuit	A2	GR6	GR4	GR2	PR2	PC18	PC18a	PC16	PC14	PC12
-	60/60	60/60	60/60	60/60	60/60	60/60	60/60	60/60	60/60	60/60
PC12	60/60	60/60	60/60	60/60	60/60	60/30	60/30	30/0	0	-
PC14	60/60	60/60	60/60	60/60	60/30	30/30	30/0	0/0	-	
PC16	60/60	60/60	60/60	60/30	30/30	30/0	0/0	-		
PC18a	60/60	60/60	60/60	60/30	30/0	0/0	-			
PC18	60/60	60/60	60/30	30/0	0/0	-				
PR2	60/60	60/30	30/0	0/0	-					

delay of the first one and its transmission to the second through the signaling system. And the fifth column shows the track circuits where both trains are located when the disturbance is produced.

The 0 value in the first column shows the moment when the second train is receiving the affectation produced by the first one (time resolution in seconds). This means that it is receiving reduced speed codes through the signaling system and these codes are in turn affecting its movement.

Increasing the T_{BT} value to obtain the $I_{DA}(T_{BT})$ characteristic curve of the station

In this step the T_{BT} of the first train is increased sequentially by increasing the Dwell Time of the first train; the results are already shown in Table 2. With this information the following curve which is characteristic of the Provença station is obtained:

The figure shows the I_{DA} value that corresponds to each T_{BT} value. The Dwell Time of the first train arriving to the station is increased sequentially. The results show that for an increase in Dwell Time of 28s the I_{DA} value reaches the minimum value of 52s. After that additional Dwell Time increments also increase the I_{DA} value until the point when the second train is fully stopped by the signaling system during its movement. Therefore, after a T_{BT} value of 33s the I_{DA} value is constant and equals to 56s.

Step 3. Using real data: Obtention of real T_{BT}, statistical analysis (frequency)

Real data coming from the installation have been used for this purpose. Those data have been acquired directly from the installation by a Moviola system, which is a computer-based device that acquires and saves continuously real-time data from the interlocking. Those data are obtained in database format and are processed using a tool created specifically for this purpose that allows filtering to acquire only the desired data. In this case, the data needed for the calculation is the status of track circuits and the ATP speed codes being injected through the coded track circuits. These codes enforce speed limits and movement authorities to allow the safety of train movements in the installation.

The indicator related to the Disturbed Running Time (T_{RD}) (which is also used to calculate the I_{DAP}) is obtained as the expected value of running times $T_R(T_{BT})$ when movements are disturbed (T_{BT} is higher than 0, therefore the second train movement is disturbed), and the frequency of real disturbance of trains f is known. The statistical frequency of T_{BT} can be found in Fig. 10.

Step 4. Indicator of disturbed capacity: Average I_{DAP} value

Using Fig. 9 which shows I_{DA} values for T_{BT} value higher than 0 and the statistical frequency of T_{BT}, the average I_{DAP} value is obtained. The I_{DAP} value equals to 57,47s. The average I_{DAP} value indicator is obtained as a result of the weighted average of all I_{DA} values by their real occurrence frequency.

$$I_{DAP} = \int_0^{INF} I_{DA}(T_{BT}) \times f(T_{BT}) d(T_{BT}) \tag{7}$$

The C_D value is calculated as follows:

$$C_D = \frac{3600}{H_D} \tag{8}$$

$$H_D = I_{DAP} + DT \tag{9}$$

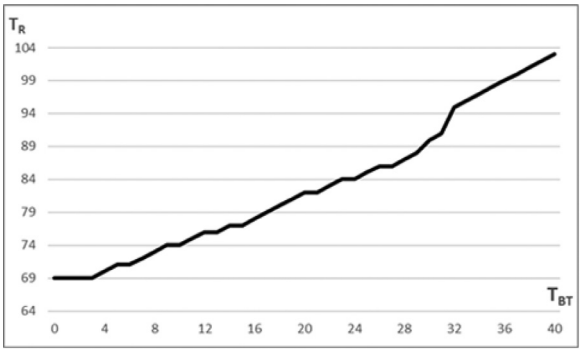

Fig. 8. $T_R(T_{BT})$ (y-axis) versus Dwell Time increase for train 1 (x-axis).

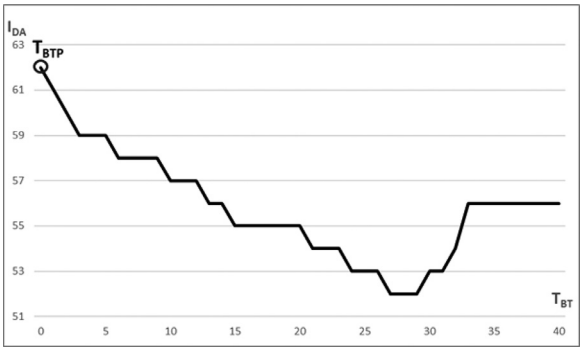

Fig. 9. I_{DA} values (y-axis) versus for T_{BT}>0.

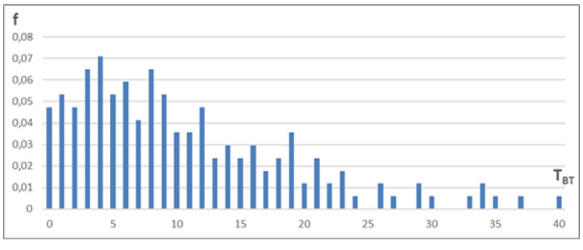

Fig. 10. Normalized statistical frequency of $T_{BT} > 0$ accumulated values (y-axis) versus Increase of Dwell Time of Train 1 (x-axis) after the T_{BTP} limit value.

$$C_D = \frac{3600}{57,47 + 30} = 41,16 \text{ Trains/Hour} \tag{10}$$

The minimum interval between trains without any disturbance is 62s. On the other hand, the I_{DAP} value for disturbed trains equals to 57.47s. This value under disturbed conditions is lower; trains move slower but also closer between each other.

Step 5. Indicator of disturbed Route Time: Average T_{RD} value

The average T_{RD} value indicator is obtained as a result of the weighted average T_{RD} values by their real occurrence frequency. It is

Table 2
Result values obtained with the simulator.

1st Train Dwell Time increase in Provença (s)T_{BT}	Departure-Arrival Interval I_{DA}	Train 2 Running Time	$-(T_{D2B} - T_{D1A})$	Train position in disturbance T1 / T2
-7	69	69	0	-
-6	68	69	1	-
-5	67	69	2	-
-4	66	69	3	-
-3	65	69	4	-
-2	64	69	5	-
-1	63	69	6	-
0	62	69	7	-
1	61	69	8	PC18 / GR4
2	60	69	9	PC18 / GR4
3	59	69	10	PC18 / GR4
4	59	70	11	PC18 / GR4
5	59	71	12	PR2 / GR6
6	58	71	13	PR2 / GR6
7	58	72	14	PR2 / GR6
8	58	73	15	PR2 / GR6
9	58	74	16	PR2 / GR6
10	57	74	17	PR2 / GR6
11	57	75	18	PR2 / GR6
12	57	76	19	PR2 / GR6
13	56	76	20	PR2 / GR6
14	56	77	21	PR2 / GR6
15	55	77	22	PR2 / GR6
16	55	78	23	PR2 / GR6
17	55	79	24	PR2 / GR6
18	55	80	25	PR2 / GR6
19	55	81	26	PR2 / GR6
20	55	82	27	PR2 / GR6
21	54	82	28	PR2 / GR6
22	54	83	29	PR2 / GR6
23	54	84	30	PR2 / GR6
24	53	84	31	PR2 / GR6
25	53	85	32	PR2 / GR6
26	53	86	33	PR2 / GR6
27	52	86	34	PR2 / GR6
28	52	87	35	PR2 / GR6
29	52	88	36	PR2 / GR6
30	53	90	37	PR2 / GR6
31	53	91	38	PR2 / GR6
32	54	95	39	PR2 / GR6
33	56	96	40	PR2 / GR6
34	56	97	41	PR2 / GR6
35	56	98	42	PR2 / GR6
36	56	99	43	PR2 / GR6
37	56	100	44	PR2 / GR6
38	56	101	45	PR2 / GR6
39	56	102	46	PR2 / GR6
40	56	103	47	PR2 / GR6

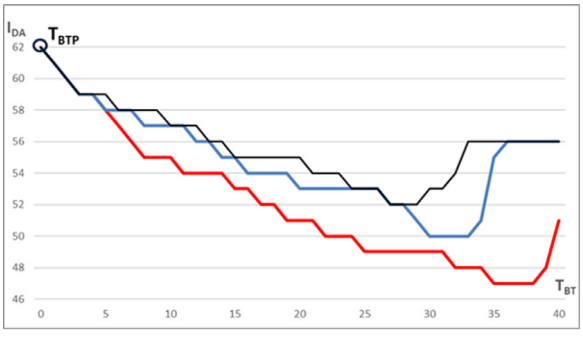

Fig. 11. I_{DA} values (y-axis) versus for T_{BT}>0, original (black), alternatives B1 (blue) and B2 (red).

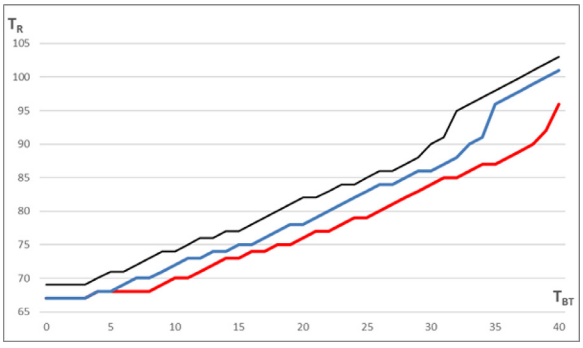

Fig. 12. $T_R(T_{BT})$ (y-axis) versus Dwell Time increase for Train 1 (x-axis), original (black), alternatives B1 (blue) and B2 (red).

calculated using:

$$T_{RD} = \int_0^{INF} T_R(T_{BT}) \times f(T_{BT}) d(T_{BT}) \quad (11)$$

The minimum T_{RD} between trains without any disturbance is 69s. When train movements are disturbed T_{RD} value equals to 75.07s. These values show the reduction in commercial speed caused by the distur-

Table 3
Braking distances in meters required to stop the train by levels of track declivity. Values include the level of additional safety applied by the operator.

	92 km/h	62 km/h	46 km/h	31 km/h	21 km/h
-25‰	572.6	303.3	195.4	116.7	76.4
0‰	457.7	243.6	157.7	95.2	63.2

bances to train movements. These disturbances show up in reduced speed codes received by the trains running too close to each other.

4.2. Design improvements

Considering the results of the application to the case study, the track layout information and the following data obtained from the brake distance table:

Declivity value in the track section to be redesigned is -25‰. This value is necessary to calculate the distance required to stop the train from every speed value until complete stop. The distance necessary depends heavily on the declivity values, hence they have to be considered.

Option A: Modification of track speed codes without any other additional change

This is the ideal solution as it is relatively the cheapest to be implemented. It only requires an interlocking software update without any change to other track or lineside systems. To check its feasibility, the proper design of the ATP design has to be revised.

- **Case a:** In this case we should check if a 60/0 reduction could fit in GR2 where we have now a 30/0 one. According to Table 3, that is not possible as we would need a brake distance of 303,3m which is longer than the length of PR2 (120.2m).
- **Case b:** In this case we should check if a 60/0 reduction could fit in GR4 where we have now a 30/0 one. According to Table 3, that is not possible as we would need a brake distance of 303,3m which is longer than the length of GR2 (192m).

Therefore, a solution only modifying the ATP speed codes design is not feasible, so this redesign option is discarded.

Option B: Change in the interlocking software and redesign the length of track circuits GR2, GR4 and GR6.

To redesign this section, we need to consider the distance required by the train to brake from every speed value until complete stop. Those values are shown in Table 3. Taking them into account, we can try to adjust the length of the track circuits to improve the efficiency of the codes applied.

Technical Discussion: In this case, in the event of an emergency brake at the end of GR2 when there is a 30/0 code (previous train in PC18), the train requires 116,7m to brake completely. The reduction 60/0 requires 303.3m, which is a value higher than the combined distance of GR2 and PR2. The following table shows the actual distances presents in the track layout:

Redesign alternatives: There could be several different redesign alternatives to be applied in this situation.

Alternative B1: In order to optimize the breaking distances design; GR2 could be reduced to 186,6m (303.3m-116.7m).

So according to these calculations, a better design of this section would be to approach the frontiers between track circuits PR2 and GR2 towards the Provença platform by a distance of 3.5m and also between track circuits GR2 and GR4 by a distance of 8.9m. The later modification will also imply moving the signal 102 accordingly.

Alternative B2: In this case, a train applying emergency brake at the end of GR4 and entering GR2 at 30km/h would require 116.7m to stop completely, which is a distance shorter than the 186.6m currently present in GR2. But this reduction is not feasible if we want to keep the reduction defined in alternative B1; which is reducing from 60/0 in GR2+PR2.

Also, a train applying emergency brake at the end of GR6 and entering GR4 at 60km/h would require 303.3m to stop completely, which is a distance shorter than the 345m currently present in GR4+GR2. Therefore, GR4 could be optimized by making the length of GR2+GR4 equal to 303.3m.

So according to these calculations the frontier between GR4 and GR6 should be moved towards Provença platform by a distance of 50.6m. This in turn would increase the length of track circuit GR6 up to 222m.

Selection between alternatives: Both alternatives displayed would allow trains to run closer in this section under disturbed conditions. Alternative B2 implies some additional works to modify track circuit limits; therefore, it needs to be evaluated if this additional investment makes sense from the operation point of view.

After these modifications, the characteristic curves obtained are the following:

The C_D value is calculated as follows:

$$C_D = \frac{3600}{H_D} \tag{12}$$

$$H_D = I_{DAP} + DT \tag{13}$$

$$C_{DB1} = \frac{3600}{56,91 + 30} = 41,42 \tag{14}$$

$$C_{DB2} = \frac{3600}{55,47 + 30} = 42,12 \tag{15}$$

The following table shows the comparison between the base and redesign alternatives B1 and B2:

Both alternatives proposed improve the performance parameters of the original design. Specifically, B2 reduces I_{DAmin} in 9.61%, I_{DAp} in 3.48%, T_{RD} in 5.33% and C_D improves in 2.33%. These performance figures are superior to the ones obtained by alternative B1, but they require a further modification in the track layout which is the displacement of the frontier between track circuits GR4 and GR6. This displacement implies the rail welding in the present position of the isolating joints to move them to their new position in the track where their installation will take place. Also, all cabling related to the track circuit connection to the rails needs to be displaced to its new position. Therefore, alternative B2 is a solution more expensive than B1 although it provides better performance. These indicators allow deciding which is the most interesting solution to be implemented in terms of its cost-efficiency and added value to the performance of the installation. In some cases, little indicator improvements require a high cost of implementation and hence may not be recommended because that money could be better spent in another point of the installation where its impact on system performance is going to be much higher. In many cases, even small percent improvements are beneficial when the line is highly saturated during the rush hour.

5. Conclusions

The railway line Barcelona-Vallès of the Spanish operator FGC is of great importance to the metropolitan region of Barcelona. The increase in passenger demand puts more pressure on the capacity of the line thus all possibilities need to be explored in order to squeeze more capacity from the current signaling system before getting involved in costly infrastructure upgrades.

In general, Railway capacity increase is one of the great challenges faced by planners and infrastructure managers. To allow them to choose the most cost-effective solution among different alternatives it becomes vital to have suitable tools available. In this article, two different indicators have been presented. These indicators ease the decision process among different installation alternatives. The indicator I_{DAP} is a measure of capacity under disturbed conditions; it is the expected value for the departure-arrival interval of trains in a node. On the other hand, the indicator T_{DM} represents the loss of commercial speed caused by the

Table 4
Original ATP design: shunting PC18 & PR2.

Shunted Track Circuit & Length	GR6 171.6m	GR4 158.4m	GR2 192m	PR2 120.2m	PC18 109m	PC18a 87m
Case a: PC18	60/60	60/30	30/0	0/0		
Case b: PR2	60/30	30/0	0/0			

Table 5
Original ATP design: shunting PC18.

Shunted Track Circuit & Length	GR6171.6m	GR4158.4m	GR2192m	PR2120.2m	PC18109m	PC18a87m
Train shunting PC18	60/60	60/30	30/0	0/0		

Table 6
Modified track circuit distances: shunting PC18.

Shunted Track Circuit & Length	GR6171.6m	GR~~4158.4m~~167,3m	GR~~2192m~~186.6m	PR~~2120.2m~~116.7m	PC18109m	PC18a87m
Train shunting PC18	60/60	60/30	30/0	0/0		

Table 7
Modified track circuit distances: shunting PR2.

Shunted Track Circuit & Lenght	GR6~~171.6m~~222m	GR4~~158.4m~~116.7m	GR~~2192m~~186.6m	PR~~2120.2m~~116.7m	PC18109m	PC18a87m
Case a2: PR2	60/30	30/0	0/0			

Table 8
Comparison of indicators between the original and redesigned cases.

Indicator	**Original**	**Alternative B1**	**Alternative B2**
$\mathbf{I_{DAmin}}$	52	50	47
$\mathbf{I_{DAp}}$	57.47	56.91	55.47
$\mathbf{T_{RD}}$	75,07	72,56	71,07
$\mathbf{C_D}$	41.16	41.42	42.12

speed reduction generated in the signaling system to protect routes of other trains in the installation or other constraints.

A case study with the application of the described model and its indicators has been presented in this work. The results show a reliable technique that can be used to improve the signaling of railway systems in order to increase its capacity levels. In Table 8 are presented the compared values between the original case and the proposed resignaling solution discussed in section 2.4. The redesigned proposal clearly improves the values of I_{DAmin} and I_{DAp}. Also, T_{RD} and C_D value are clearly improved. All these changes enable more capacity in the section without the implementation of expensive changes, just with the displacement of three track circuits separation zones.The aforementioned indicators presented can be used to improve decisions taken in the field of design and redesign of signaling systems and therefore support the cost-benefit analysis process previous to a sound infrastructure investment. There are many application possibilities available, from choosing between different signaling design alternatives by applying the indicators from scratch in Greenfield projects to selecting the most cost-effective solution to increase capacity in Brownfield Projects. The next steps in this investigation should be to extend the application to other urban and suburban installations to increase the collection of results obtained. This would lead to an even better comprehension of the presented method.

Availability of data and material

The data input used for this project simulations belongs to FGC, a Spanish railway operator. Sharing that data could breach their privacy policies.

Funding

No external funding was received for this project.

Authors' contribution

LMN carried out the simulations, study design and data analysis, also draft the full manuscript. AFC and APC participated in the overall proposal of the idea and also the design of the study and simulations. All authors read and approved the final manuscript.

Declaration of Competing Interest

Not applicable.

Acknowledgements

Not applicable.

References

Abril, M., Barber, F., Ingolotti, L., Salido, M. A., Tormos, P., & Lova, A. (2008). An assessment of railway capacity. *Transportation Research Part E: Logistics and Transportation Review, 44*(5), 774–806.

Becker, M., & Schreckenberg, M. (2018). Case study: influence of stochastic dwell times on railway traffic simulations. In *IEEE Conference on Intelligent Transportation Systems, Proceedings, ITSC, 2018-Novem(5550)* (pp. 1227–1233). 10.1109/ITSC.2018.8569934.

Burdett, R. L. (2016). Optimisation models for expanding a railway's theoretical capacity. *European Journal of Operational Research, 251*(3), 783–797. 10.1016/j.ejor.2015.12.033.

Gašparík, J., Abramović, B., & Zitrický, V. (2018). Research on dependences of railway infrastructure capacity. *Tehnicki Vjesnik, 25*(4), 1190–1195. 10.17559/TV-20160917192247.

Goverde, R. M. P., Corman, F., & D'Ariano, A (2013). Railway line capacity consumption of different railway signalling systems under scheduled and disturbed conditions. *Journal of Rail Transport Planning and Management, 3*(3), 78–94.

Haramina, H., & Talan, I. (2018). Improvement of suburban railway services by infrastructure and timetable modifications based on simulation modelling. *Transport Problems, 13*(3), 15–27. 10.20858/tp.2018.13.3.2.

Huang, P., Wen, C., Peng, Q., Jiang, C., Yang, Y., & Fu, Z. (2019). Modeling the influence of disturbances in high-speed railway systems. *Journal of Advanced Transportation, 2019*(2), 1–13. 10.1155/2019/8639589.

Jensen, L. W., Landex, A., Nielsen, O. A., Kroon, L. G., & Schmidt, M. (2017). Strategic assessment of capacity consumption in railway networks: Framework and model. *Transportation Research Part C: Emerging Technologies, 74*, 126–149. 10.1016/j.trc.2016.10.013.

Ljubaj, I., Mlinarić, T. J., & Radonjić, D. (2017). Proposed solutions for increasing the capacity of the mediterranean corridor on section Zagreb - Rijeka. *Procedia Engineering, 192*, 545–550. 10.1016/j.proeng.2017.06.094.

Ljubaj, I., Mlinarić, T. J., Lezaić, T., & Starčević, M. (2018). The possibility of capacity increase on the modernised and electrified railway line R201 along the Zaprešić-Zabok section. *MATEC Web of Conferences, 235*, 8–11. 10.1051/matecconf/201823500009.

Ljubaj, I., & Mlinarić, T. J. (2019). The possibility of utilising maximum capacity of the double-track railway by using innovative traffic organisation. *Transportation Research Procedia, 40*, 346–353. 10.1016/j.trpro.2019.07.051.

Luteberget, B., Claessen, K., & Johansen, C. (2019). Design-time railway capacity verification using SAT modulo discrete event simulation. In *2018 Formal Methods in Computer Aided Design (FMCAD)* (pp. 1–9). 10.23919/fmcad.2018.8603003.

Nalmpantis, D., Roukouni, A., Genitsaris, E., Stamelou, A., & Naniopoulos, A. (2019). Evaluation of innovative ideas for Public Transport proposed by citizens using Multi-Criteria Decision Analysis (MCDA). *European Transport Research Review, 11*(1). 10.1186/s12544-019-0356-6.

OECD/ITF. (2017). *ITF Transport Outlook 2017*. Paris: OECD Publishing http://dx.doi.org/10.1787/9789282108000-en.

Nash, A, & Huerlimann, D (2004). Railroad simulation using OpenTrack. *Computer Railway, IX*, 45–54.

Reinhardt, L. B., Pisinger, D., & Lusby, R. (2018). Railway capacity and expansion analysis using time discretized paths. *Flexible Services and Manufacturing Journal, 30*(4), 712–739. 10.1007/s10696-017-9292-8.

Shekhar, S., Singh, A., Belur, M. N., & Rangaraj, N. (2019). Development of a railway junction simulator for evaluation of control strategies and capacity utilization optimization. In *2019 5th Indian Control Conference, ICC 2019 - Proceedings, (Icc)* (pp. 260–265). 10.1109/INDIANCC.2019.8715629.

Zhong, M. (2018). Analyzing and evaluating infrastructure capacity of railway passenger station by mesoscopic simulation method. In *2018 International Conference on Intelligent Rail Transportation (ICIRT)* (pp. 1–5). 10.1109/ICIRT.2018.8641593.

Zieger, S., Weik, N., & Nießen, N. (2018). The influence of buffer time distributions in delay propagation modelling of railway networks. *Journal of Rail Transport Planning and Management, 8*(3–4), 220–232. 10.1016/j.jrtpm.2018.09.001.

Luis Miguel Navarro received the Industrial Engineering degree from the Universitat Politècnica de Catalunya, Terrassa, in 2007 and the Business Management degree from the Universitat Oberta de Catalunya, Barcelona, in 2014. He also received the PhD degree in 2020 from Comillas Pontifical University. He joined Siemens Rail Automation in 2010 and works as a certified Project Manager in Barcelona. He has been engaged in design and installation of signaling systems since 2010. His research interests include train simulation, railway capacity analysis and fuzzy systems.

Antonio Fernández-Cardador received the Physics degree from the Universidad Complutense de Madrid, Madrid, Spain, in 1991 and the Ph.D. degree from Comillas Pontifical University, Madrid, in 1997. He is a Research Fellow at the Railways Research Group, Institute for Research in Technology, and a Full Professor at ICAI School of Engineering, Comillas Pontifical University. His research interests include train simulation, railways operation and control, eco-driving, and railway capacity.

Asunción P. Cucala received the Electrical Engineering and Ph.D. degrees from Comillas Pontifical University, Madrid, Spain, in 1995 and 2003, respectively. She is a Research Fellow at the Railways Research Group, Institute for Research in Technology, and an Assistant Professor at ICAI School of Engineering, Comillas Pontifical University. Her research interests include energy efficiency in railways, railway capacity analysis, train simulation, and railways operation and control.